Pediatric Radiology (2019) 49:1823–1839
https://doi.org/10.1007/s00247-019-04494-2

PICTORIAL ESSAY

Dual-source computed tomography coronary artery imaging in children

Aurelio Secinaro[1] · Davide Curione[1] · Kristian Havmand Mortensen[2] · Teresa Pia Santangelo[1] · Paolo Ciancarella[1] · Carmela Napolitano[1] · Alessia Del Pasqua[3] · Andrew Mayall Taylor[4] · Paolo Ciliberti[3]

Received: 28 September 2018 / Revised: 11 June 2019 / Accepted: 1 August 2019 / Published online: 22 August 2019

Abstract

Computed tomography (CT) has a well-established diagnostic role in the assessment of coronary arteries in adults. However, its application in a pediatric setting is still limited and often impaired by several technical issues, such as high heart rates, poor patient cooperation, and radiation dose exposure. Nonetheless, CT is becoming crucial in the noninvasive approach of children affected by coronary abnormalities and congenital heart disease. In some circumstances, CT might be preferred to other noninvasive techniques such as echocardiography and MRI for its lack of acoustic window influence, shorter acquisition time, and high spatial resolution. The introduction of dual-source CT has expanded the role of CT in the evaluation of pediatric cardiovascular anatomy and pathology. Furthermore, technical advances in the optimization of low-dose protocols represent an attractive innovation. Dual-source CT can play a key role in several clinical settings in children, namely in the evaluation of children with suspected congenital coronary artery anomalies, both isolated and in association with congenital heart disease. Moreover, it can be used to assess acquired coronary artery abnormalities, as in children with Kawasaki disease and after surgical manipulation, especially in case of transposition of the great arteries treated with arterial switch operation and in case of coronary re-implantation.

Keywords Children · Congenital heart disease · Coronary artery anomalies · Coronary artery imaging · Dual-source computed tomography · Heart

Introduction

Coronary artery imaging is often challenging in children because of problems related to small size, high heart rates, motion artifacts from cardiac movement and respiration, and limited patient cooperation. Therefore, high spatial and temporal resolution, short examination time and low patient risks are required in children [1]. Imaging modalities for evaluating coronary arteries in children include echocardiography, conventional invasive angiography, MRI and CT. Transthoracic echocardiography is widely used as the primary imaging approach [2]. However it is impaired by its limited utility for fully characterizing coronary anatomy, by poor acoustic windows, and by operator-dependency. Conventional angiography can provide both anatomical and functional information, particularly in children with congenital heart disease, but it is associated with non-negligible risks related to its intrinsic invasiveness and to the use of potentially high doses of ionizing radiation and iodinated contrast agent [3]. Thus it should be reserved for interventional procedures or when noninvasive diagnostic imaging is inconclusive. MRI also provides information on cardiac anatomy and function, allowing for 3-D coronary artery imaging without the use of ionizing radiation. However, it is impaired by long acquisition time requiring prolonged patient cooperation, which might not be possible in children without general anesthesia, and by limited spatial resolution [4], which makes coronary evaluation beyond origin assessment difficult.

✉ Aurelio Secinaro
aurelio.secinaro@opbg.net

[1] Advanced Cardiovascular Imaging Unit – Department of Imaging, Bambino Gesù Children's Hospital, IRCCS, Rome, Italy

[2] Cardiorespiratory Unit, Great Ormond Street Hospital for Children, London, UK

[3] Pediatric Cardiology and Cardiac Surgery Department, Bambino Gesù Children's Hospital, IRCCS, Rome, Italy

[4] UCL Centre for Cardiovascular Imaging, Institute of Cardiovascular Science, University College of London, Great Ormond Street Hospital for Children, London, UK

CT is considered the diagnostic method of choice for non-invasive coronary artery imaging. Recently it has undergone significant advances in the technical field and, especially with the advent of dual-source CT and modern strategies to reduce radiation dose, it has been used more frequently to evaluate coronary arteries and complex congenital heart disease in children [5]. At present, several congenital and acquired coronary artery abnormalities can be accurately and safely described by CT in the pediatric population.

Technical aspects

Each cardiac CT exam should be tailored to the individual child to maximize diagnostic information and minimize risk. Compared to most other indications in congenital heart disease, optimal coronary artery imaging requires higher image quality, implying the highest spatial and temporal resolution available, possibly associated with slow and regular heart rate and breath-holding [6]. State-of-the-art second- and third-generation dual-source CT scanners (SOMATOM Definition Flash and SOMATOM Force, respectively, Siemens Healthineers, Erlangen, Germany; Table 1) allow for submillimeter isotropic imaging of the heart and coronary arteries in one or a few heart beats, paired with dose-reduction techniques including high-pitch spiral scanning, low tube voltage acquisition, and iterative reconstruction [7]. At our center, we perform all CT exams using a second-generation dual-source CT scanner.

Patient preparation

Children should be carefully positioned on the CT table at the isocenter of the scanner in the supine position, with the arms above the head and with electrocardiography electrodes outside the thoracic region, on the arms and upper abdomen, to prevent image-quality deterioration (i.e. beam-hardening artifacts) or radiation dose increase [8]. Thanks to the versatility of dual-source CT, most exams can be performed without sedation or anesthesia. Although minor motion artifacts might not significantly alter image quality [9], it is important to ensure children remain still during scanning. If they are unable to cooperate or become agitated, various solutions can be adopted [10].

Generally, only information on the proximal or anatomical course of the coronary arteries is requested in children; therefore they can be scanned free-breathing if they are unable to follow instructions [11], even at high heart rates, because there is limited motion of the proximal coronary vessels throughout the cardiac cycle. Free-breathing scanning is one the most notable advantages of dual-source CT. However, when distal or detailed coronary artery imaging is needed, breath-holding is beneficial. If children are compliant, practicing the breath-hold before the exam helps to maximize cooperation and assess respiratory sinus arrhythmia. Otherwise, anesthesia with suspended respiration can be considered [6]. For the same reasons, nitrates and beta-blockers are often not needed to evaluate the coronary arteries in children given that they prolong patient preparation time with no guaranteed success [12]. Nevertheless, they have been shown to be safe in children [13] with careful screening for contraindications and should be considered [14, 15] if high-definition imaging is required, particularly beta-blockers, because image quality and radiation reduction algorithms remain heart-rate-dependent.

Contrast injection

Iodinated contrast agent is usually injected via a peripheral vein using a dual-syringe power injector [16]. Intravenous line size is affected by the site of cannulation and body size,

Table 1 Main technical specifications for second- and third-generation dual-source CT scanners

Characteristics	Second-generation (SOMATOM Definition Flash)	Third-generation (SOMATOM Force)
Number of detector rows	128 (64×2)	192 (96×2)
Detector z-dimension	0.6 mm	0.6 mm
Rotation time	0.28 s	0.25 s
Temporal resolution	75 ms	66 ms
Spatial resolution	0.30 mm	0.24 mm
Z-axis coverage	38.4 mm	57.6 mm
Maximum scan speed	458 mm/s (Flash)	737 mm/s (Turbo Flash)
Field of view	Main tube: 50 cm	Main tube: 50 cm
	Secondary tube: 33 cm	Secondary tube: 35 cm
Kilovoltage settings (kV)	70, 80–140 in steps of 20	70–150 in steps of 10
Iterative reconstruction	SAFIRE	ADMIRE

ADMIRE advanced modeled iterative reconstruction, *SAFIRE* sinogram affirmed iterative reconstruction

typically ranging from 24-gauge (G) in neonates to 18-G in older children, with flow rates between 0.5 mL/s and 5 mL/s [17] and pressure settings of 50–300 pounds per square inch (psi). Central venous catheters might also be used for contrast infusion, especially in critically ill children, but they might only allow for adequate injection in younger children because they generally have lower maximum flow rates and psi values [18] (0.4–1.2 mL/s and 25–50 psi) or require hand injection.

Contrast concentration and volume should be adapted to the intravenous access and body weight, employing 300–400 mgI/mL agents at 1–3 mL/kg until standard adult contrast agent amounts are reached. Lower concentrations with higher volumes are typically used in infants and younger children with smaller intravenous lines or with central venous catheters, whereas higher concentrations with lower volumes are usually infused in older children and adolescents with larger cannulas (Table 2). Special care must be taken to avoid accidental injection of air, which can result in paradoxical embolism in the presence of intra-cardiac shunting.

The most common injection protocols include a biphasic or triphasic approach [6]. The biphasic protocol consists of contrast administration followed by a saline bolus, timing image acquisition to opacification of the ascending aorta. This is the usual method for coronary artery imaging if there are no associated cardiovascular lesions. The triphasic protocol entails a two-phase contrast infusion (about half at the regular rate plus the remainder either at a slower rate or as a contrast/saline mix) [19] followed by a saline flush. This is most frequently used in the presence of associated cardiovascular lesions to obtain simultaneous evaluation of right- and left-side structures.

Scan timing

On the one hand, a fixed time can be set to initiate scanning at the end of the injection protocol (typically about 20 s). The site of cannulation and scan protocol should be considered, with additional delay when injecting from the leg and earlier acquisition when using longer scan methods. This approach might be best suited for infants and younger children because it avoids unnecessary radiation exposure related to the use of bolus monitoring scans. Besides, for many indications contrast opacification need not be as high as in conventional adult coronary imaging. Nevertheless, this method is challenging because it is prone to inaccuracy and limited reproducibility from the variability of contrast transit time for technical and anatomical/functional reasons, particularly in children with single-ventricle physiology, valvular pathology or ventricular dysfunction [6].

Table 2 Recommendations for contrast administration

Intravenous line		Power injection		Contrast agent	
Type	Size	Flow rate	Pressure	Concentration	Volume
Central	Any	≤1.5 mL/s	≤50 psi	≤350 mgI/mL	2–3 mL/kg
Peripheral	24-G	≤1.5 mL/s	50–100 psi		
	22-G	≤3.0 mL/s	100–200 psi		
	20-G	≤5.0 mL/s	300 psi	≤400 mgI/mL	1–2 mL/kg
	18-G	≤6.5 mL/s	300 psi		

G gauge, *psi* pounds per square inch

On the other hand, bolus-monitoring techniques enable scanning at optimal opacification and are especially useful in older children with higher inter-variability [17]. The test-bolus approach consists of administering a small amount of contrast agent and calculating vascular peak enhancement time by monitoring contrast transit on a target slice. An extra delay (usually 3–6 s) must be added in the actual acquisition depending on various factors (e.g., body size, scan protocol) [20]. Because this method involves additional contrast agent and radiation exposure, it is not routinely used in children. With the bolus-tracking technique, the scan is triggered when vascular enhancement reaches an adequate level in a structure of interest monitored on a target slice [21]. Automatic triggering, using a region of interest with a Hounsfield unit (HU) threshold (e.g., 150 HU at 100 kV, with higher thresholds for lower kV), can be difficult in children given the risk of errors from the combination of small vascular structures and potential movement. Manual initiation with a visual approach more reliably ensures ideal opacification, especially in the context of complex congenital heart disease where contrast agent might not follow the expected route. To reduce radiation exposure, monitoring should start near the end of contrast injection and should be reduced in frequency, and both tube power and current should be decreased [10].

Scan protocol

The scan range should include the heart for standard coronary imaging but might need to be extended to the ascending aorta/pulmonary arteries or further depending on the clinical indication, especially in the context of congenital heart disease. The main acquisition methods include prospective electrocardiography (ECG)-triggered high-pitch dual-source spiral, prospective ECG-gated sequential, and retrospective ECG-gated spiral scanning. Prospective ECG-triggered high-pitch dual-source spiral scanning (turbo Flash), distinct to dual-source CT, uses both X-ray tubes within the scanner to achieve both maximum temporal resolution and z-axis scan speed, resulting in rapid and large gapless non-overlapping imaging in a single heartbeat with a limited field of view (corresponding to that of the secondary tube). Data acquisition is prospectively triggered by the ECG so that subsequent images are obtained at progressively later times within the cardiac cycle [22]. This means the dataset is not uniform in time and cannot be ECG-edited, contrary to sequential and retrospective ECG-

synchronized scans. This method can provide accurate evaluation of the whole coronary tree using diastolic triggering in children with regular heart rates below 60–65 beats per minute (bpm). Nevertheless it can also be used at higher heart rates with end-systolic triggering to visualize proximal coronary course, although motion artifacts might occur, especially at the end of the scanned volume. Additionally, this method is particularly recommended in cases of uncooperative children because it reduces respiratory and cardiac motion artifacts, as well as the need for sedation and general anesthesia [11].

When there is need for extended anatomical coverage in combination with coronary assessment, it might be appropriate to use a protocol that allows for scanning a large volume in the high-pitch modality with a prospective ECG-triggered box targeted at the level of the heart or, if only proximal coronary course is required, at the level of the aortic root (Fig. 1). High accuracy in the evaluation of intracardiac structures and coronary arteries with only minor image-quality deterioration has been reported for the high-pitch acquisition [5]. Several studies in the literature have shown lower radiation doses compared to the prospective ECG-gated sequential method, with a mean effective radiation dose of about 0.2–0.5 mSv [23, 24].

In prospective ECG-gated sequential (step-and-shoot) and retrospective ECG-gated spiral scanning, imaging occurs with acquisition of a portion or the entire R-R interval, respectively, to find the best resting period for each coronary artery [17]. Both X-ray tubes are still employed to achieve maximum temporal resolution over multiple heartbeats without field-of-view limitation. The sequential method is especially recommended for detailed assessment of the coronary tree, particularly in cooperative children with higher or irregular heart rates. A drawback is the possibility of stack artifacts, which seldom seriously affect image interpretation in children. Prospective scanning still entails low radiation dose, especially when compared to retrospective scanning, with a mean effective dose of 0.3–1.0 mSv [17, 25]. Besides, the high temporal resolution of dual-source CT has drastically reduced the need for the retrospective technique, particularly for high-dose protocols with multi-segment reconstruction, which are necessary at high heart rates with single-source scanners. Moreover, although retrospective scanning can be obtained at relatively low radiation dose (mean effective dose approximately 2–5 mSv) [17, 26] thanks to several strategies, namely the use of intensive pulsing modulation and higher pitch values at higher heart rates, it should be considered in select cases, especially when looking for detailed coronary imaging with challenging elevated and highly irregular heart rhythm or when seeking dynamic information, such as valvular motion or ventricular function [10]. Figure 2 outlines suggestions for protocol selection [27–29].

All CT examinations should employ a low-dose protocol, including weight-adapted settings for tube voltage (80 kV in children under 40 kg [consider 70 kV in neonates/infants]; 100 kV in children larger than 40 kg [consider 120 kV in overweight/high-density patients]) and current (10 mAs/kg in children under 5 kg, 4–5 mAs/kg up to 92 mAs in children 6–15 kg, and 2–3 mAs/kg up to 138 mAs in children larger than 15 kg) [30]. Another strategy to reduce radiation dose is (semi-)automatic modulation of tube voltage and current [5, 31].

Compared to other state-of-the-art technology, namely 256- and 320-row scanners, dual-source CT has unparalleled temporal resolution (66–75 ms versus at least 140 ms), resulting in motion-free imaging even at the high heart rates of children. On the other hand, 256- and 320-row machines are capable of greater z-axis coverage in one gantry rotation (160 mm versus 38.4–57.6 mm of dual-source CT), allowing for acquisition of the whole heart in a single heartbeat, thus reducing misregistration artifacts and contrast volume [32]. This can also be achieved by dual-source CT in the prospective high-pitch mode, even if low heart rates are required for high-definition imaging. Finally, radiation dose is similar among scanners [33, 34], though with lowest values for the high-pitch technique.

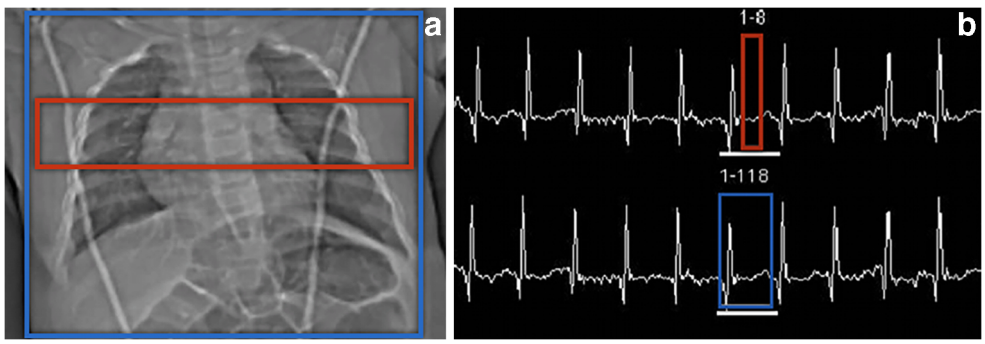

Fig. 1 High-pitch spiral protocol with prospective electrocardiography (ECG)-triggered box. **a** Anteroposterior scanogram shows the large non-triggered chest volume (*blue square*) with the smaller prospective ECG-triggered box (*red square*) at the level of the aortic root. **b** ECG report indicates the chest (*blue square*) and coronary (*red square*) acquisition windows with respect to the R-R interval. Coronary scan is set at end-systole, in accordance with the high heart rate (106 beats per minute)

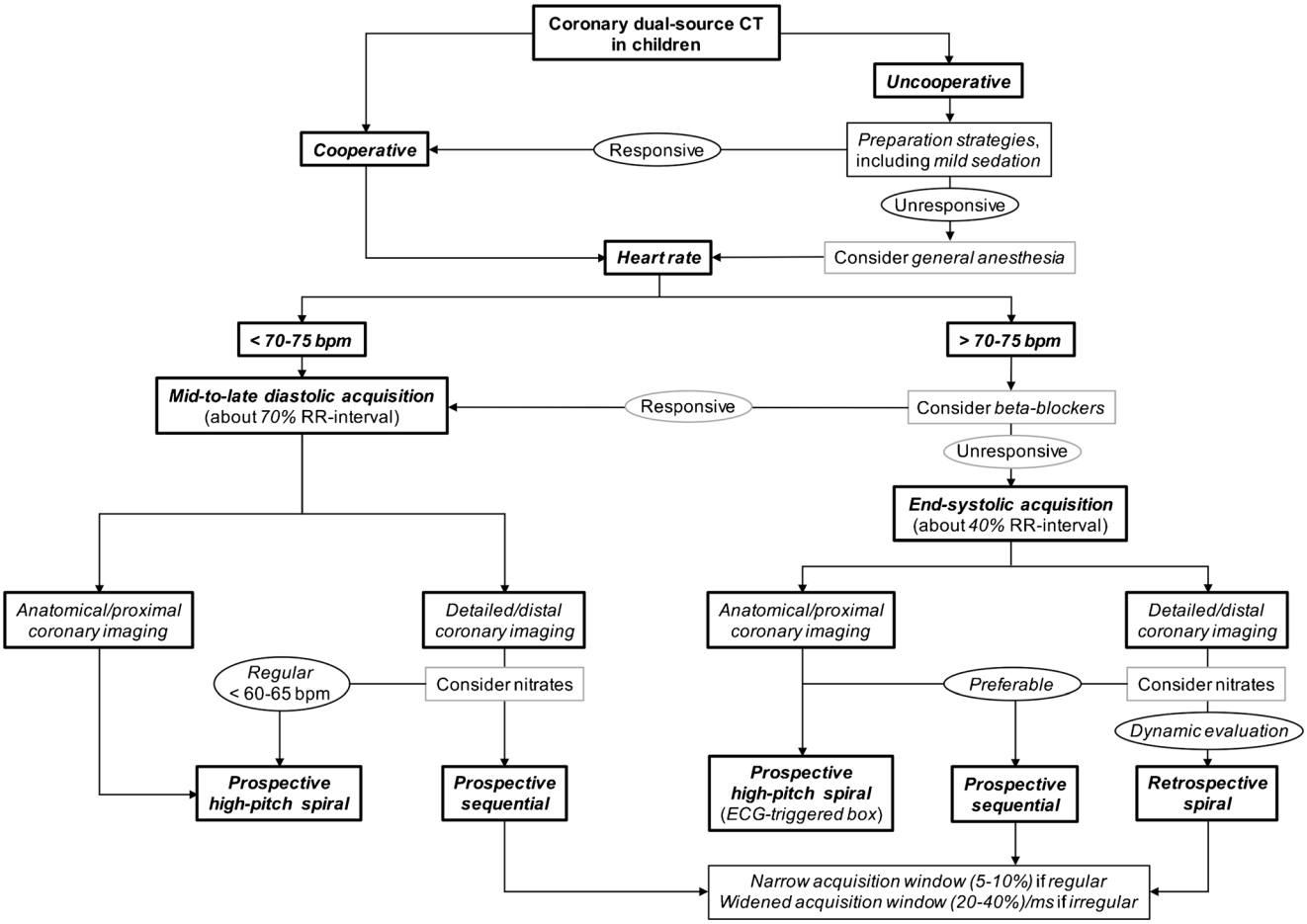

Fig. 2 Suggestions for dual-source CT protocol selection for coronary artery imaging in children. There are three main stages. The first step consists of assessing patient compliance. Various strategies can be employed in uncooperative children to avoid general anesthesia: physical immobilization devices (i.e. soft weights, restraining bands or vacuum cushion [10]); swaddling and scanning while sleeping, especially after eating ("feed-and-wrap" technique), oral glucose, or pacifiers in infants; and parent/tutor or audio/video support in young children. If necessary, mild sedation with short-acting benzodiazepines, such as midazolam, may be administered. The second step involves evaluating heart rate to determine the best cardiac phase for coronary imaging. In general, to ensure the heart is imaged during its optimal motion-free time frame, children with lower heart rates (below 70–75 bpm) should be scanned during mid-to-late diastole (about 70% of the R-R interval), whereas children with higher heart rates (above 70–75 bpm) should be scanned at end-systole (around 40% of the R-R interval) [27]. Finally, the purpose of the exam guides protocol choice. Generally only information on proximal or anatomical course of the coronary arteries is requested in children. Prospective high-pitch spiral scanning can be used to obtain this information at low as well as high heart rates, although it might be less reliable and more indicated when coronary imaging is not the primary concern at elevated heart rhythms, especially with the electrocardiography (ECG)-triggered box at the level of the aortic root. High-definition imaging with this technique requires low and stable heart rates. Prospective sequential scanning should be the preferred method whenever the high-pitch technique is not suitable. In contrast, retrospective spiral scanning should be reserved for cases where concurrent dynamic evaluation (e.g., ventricular function) is required. In these modalities, acquisition window (or ECG pulsing) refers to the portion of cardiac cycle in which the scanner acquires data for prospective scanning or delivers maximum tube current for retrospective scanning, respectively. If the heart rate is regular, a narrow acquisition window should be used [28], typically selected as a relative percentage interval of the cardiac cycle (5–10%). In contrast, in children with significant heart rate variability, a widened acquisition window (20–40%) or millisecond scanning might be employed, making use of an adaptive algorithm of correction [29] that dynamically modifies the scanned portion of the cardiac cycle according to the frequency. Medications, namely beta-blockers and nitrates, are often not necessary for coronary artery assessment in children but should be considered to achieve high-definition imaging

Image reconstruction and interpretation

Dual-source CT raw data can be reconstructed using two techniques, filtered back-projection and iterative reconstruction. The former is the standard analytical CT method, while the latter is a noise-reducing algorithm that employs measured raw and simulated data to generate image estimates that are compared and corrected in cycles at different strength levels. The major benefit of iterative reconstruction is the possibility to reduce image noise in exams acquired with low-dose protocols, preserving image quality [35]. Also, artifacts typically associated with filtered back-projection are decreased, such as

beam-hardening or blooming artifacts arising from high-density objects like coronary stents, allowing for better delineation of vessel lumen. The combination of iterative reconstruction and low–tube voltage enables one to decrease the volume of contrast agent without reducing the image quality [30].

In prospective sequential or retrospective spiral scans, the best cardiac phase for image reconstruction can be automatically defined by the scanner, thanks to software approaches based on motion maps applied to the raw data set for automatic determination of minimal cardiac motion. If unsatisfactory, the best cardiac phase can be manually decided by the operator through multiphase evaluation, in which case it is important to reconstruct several phases to determine the best frame of cardiac rest, keeping in mind that multiple phases might be needed to fully assess the different portions of the coronary tree. In case of irregular heart rate, it might be advisable to reconstruct phases according to milliseconds rather than relative percentage intervals because this method could be superior [36]. In addition to transaxial images, the following reconstructions are recommended for image interpretation [37, 38]: multiplanar reformations in three adjustable planes, including curved planar reformations along the coronaries to display their tortuous course and vessel cross-sections for lumen evaluation when necessary; maximum-intensity projection images for "angiography-like" views, allowing for quick and intuitive visualization of coronary course; and volume-rendering reconstructions for a 3-D overview of coronary anatomy, including virtual angioscopy that can be useful to depict the coronary ostia. All these steps should be performed by clinicians (radiologists in our center) and can be time-consuming, especially in cases of high-definition imaging and complex congenital heart disease (up to 30 min to 1 h).

Clinical indications

Coronary artery abnormalities in children can be congenital or acquired. Congenital anomalies include a complex group of disorders occurring as isolated conditions or in the spectrum of congenital heart disease. Acquired coronary anomalies are mainly secondary to Kawasaki disease or surgery when congenital heart disease repair involves coronary manipulation. Increasing evidence supports the role of CT in general and dual-source CT in particular for coronary evaluation of these children [39, 40].

Congenital coronary artery anomalies

Isolated anomalies

Isolated coronary abnormalities are the second most common cause of cardiovascular death in young athletes in Europe and the United States [41]. Clinical manifestations vary, ranging from incidental findings to sudden cardiac death ("malignant" variants). Three main categories can be identified, including anomalies of origin and course, of intrinsic coronary anatomy and of termination (Table 3) [42].

Anomalies of origin and course entail variation in the number, shape and location of the coronary ostia. On the one hand, benign variants are quite common and, although not hemodynamically significant, they become relevant in cases of cardiac surgery. On the other hand, some abnormalities are associated with high mortality. In particular, anomalous origin of the left coronary artery from the pulmonary artery (Fig. 3), albeit a rare condition (1:300,000 births), can cause a coronary steal phenomenon into the pulmonary circulation with development of intercoronary collaterals, leading to myocardial ischemia, heart failure and ventricular arrhythmias from the early neonatal period [43]. A less dramatic but still potentially fatal condition is the inappropriate origin of a coronary artery with interarterial or intramural course (Figs. 4 and 5), which is particularly dangerous if it involves the left coronary artery. This pattern is often asymptomatic, but sudden death — particularly during maximal exercise — can occur. CT has a key role in these settings for confirming the diagnosis, for aiding in surgical planning when indicated and for ruling out complications after a corrective operation [44]. Specifically, CT might be superior to conventional angiography for defining the ostial origin and proximal course of anomalous coronary branches [45], providing 3-D anatomical information that can be difficult to obtain with invasive angiography and avoiding potential issues related to cannulation of anomalous coronary vessels.

Table 3 Main classes of congenital coronary artery anomalies

Anomalies of coronary origin and course	Absent left main or split origin of the left coronary artery
	Anomalous coronary ostium outside the aortic sinuses, including anomalous origin of the left coronary artery from the pulmonary artery
	Anomalous location of coronary ostium at improper sinus, including interarterial/intramural course
	Single coronary artery
Anomalies of intrinsic coronary anatomy	Congenital ostial stenosis or atresia
	Coronary ectasia and aneurysm
	Myocardial bridging
	Duplicated arteries
	Subendocardial coronary course
	Coronary crossing
Anomalies of coronary termination	Coronary artery fistulas

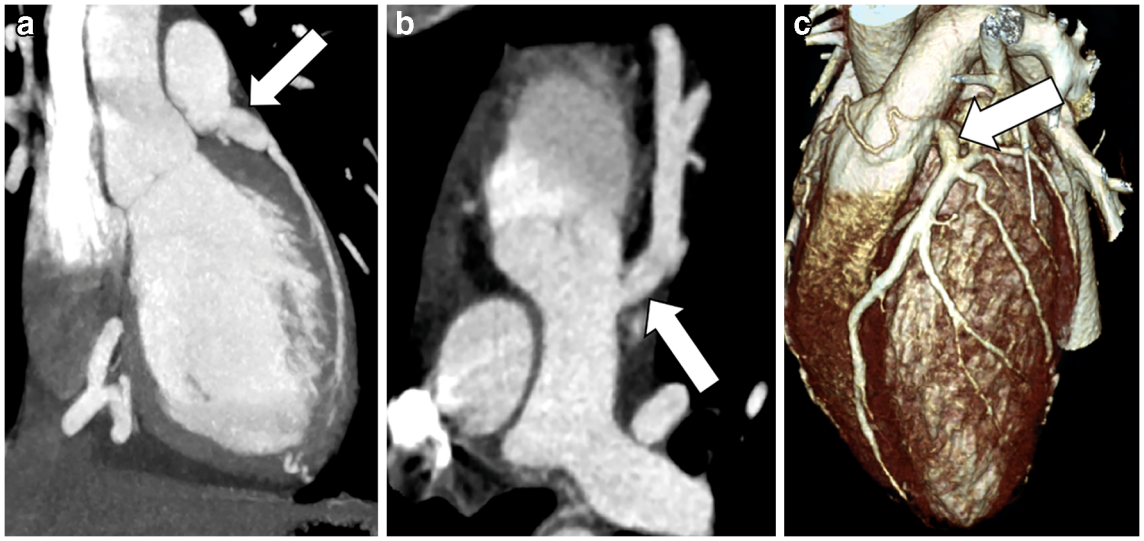

Fig. 3 Anomalous origin of the left coronary artery from the pulmonary artery in a 1-year-old girl. **a–c** Coronal maximum-intensity projection (**a**), oblique axial multiplanar reformation (**b**) and left anterior volume-rendered (**c**) CT images demonstrate that the left coronary artery (*arrows*) arises from the pulmonary trunk and is dilated, especially proximally

Myocardial bridging is a frequently encountered intrinsic coronary anomaly (frequency near 25%, range 5–86% in autoptic and imaging studies) [46], whereby a coronary artery segment shows intramuscular rather than epicardial course. All coronary tracts can be involved, but the middle left anterior descending artery seems to be the most common [47]. In myocardial bridging, the affected vascular segment can become compressed during systole, sometimes creating transitory myocardial ischemia. It has been argued that most instances are of little clinical importance; however, several reports suggest that some cases produce coronary thrombosis, myocardial ischemia and infarction, and predispose to atherosclerosis or sudden death [48, 49]. In general, myocardial bridging should be suspected in children with exertional angina but no coronary risk factors, especially if young. Compared to catheter angiography, CT clearly shows the intramyocardial location of the involved coronary segment (Fig. 6). Obtaining both systolic and diastolic phases allows for assessment of luminal narrowing throughout the cardiac cycle [45].

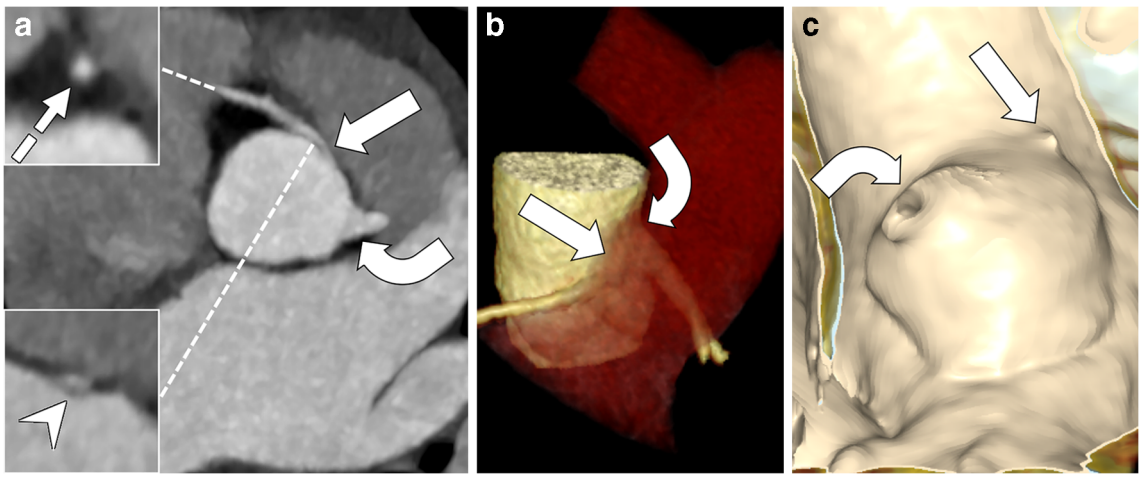

Fig. 4 Anomalous origin of the right coronary artery from improper aortic sinus in a 7-year-old boy. **a–c** Axial maximum-intensity projection with embedded vessel cross-section insets from locations indicated by dashed lines (**a**), anterior volume-rendered (**b**) and angioscopic-like (**c**) CT images demonstrate that both the right (*straight arrows*) and left (*curved arrows)* coronaries arise from the left aortic sinus. In detail, the right coronary artery has iuxta-junctional and iuxta-commissural origin with interarterial course between the aortic root and pulmonary trunk as well as high-risk imaging features, namely acute takeoff angle, slit-like orifice, and elliptical lumen proximally (*arrowhead*), consistent with intramural segment. Vessel lumen returns circularly more distally (*dotted arrow*)

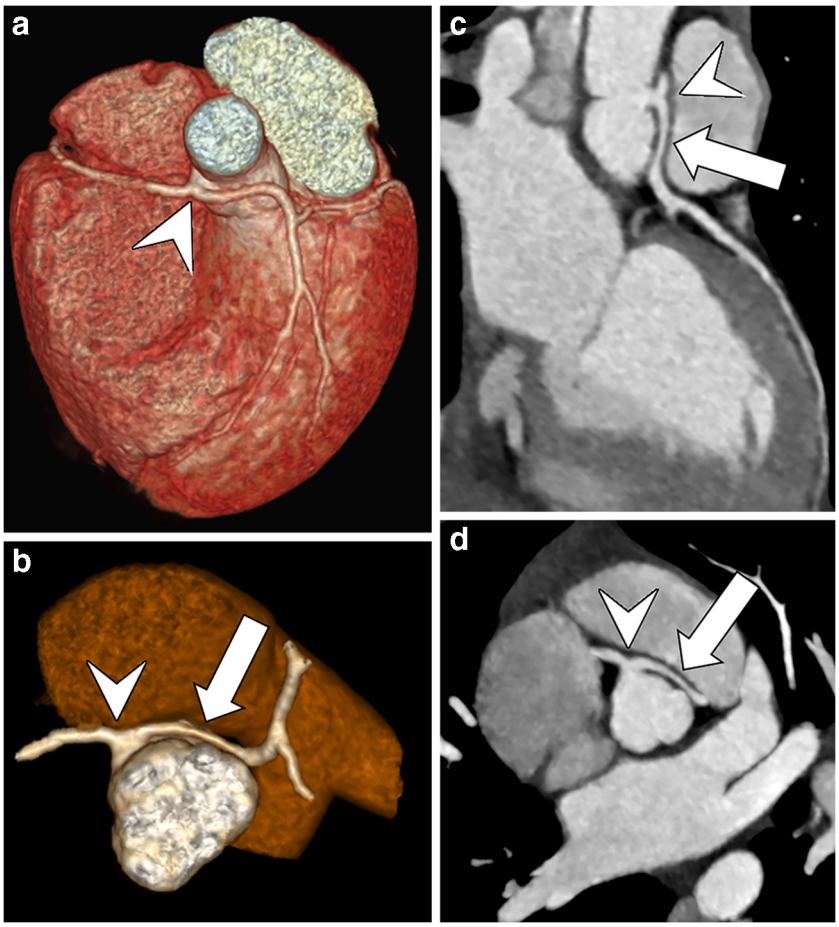

Fig. 5 Anomalous origin of the left coronary artery in a 12-year-old boy. **a–d** Anterior oblique (**a**) and inferior (**b**) volume-rendered, curved planar reformation (**c**) and axial maximum-intensity projection (**d**) CT images demonstrate that the left coronary artery originates from the opposite (right) sinus of Valsalva, with a shared ostium (*arrowhead*) with the right coronary artery. The left main coronary artery also shows interarterial course (*arrow*)

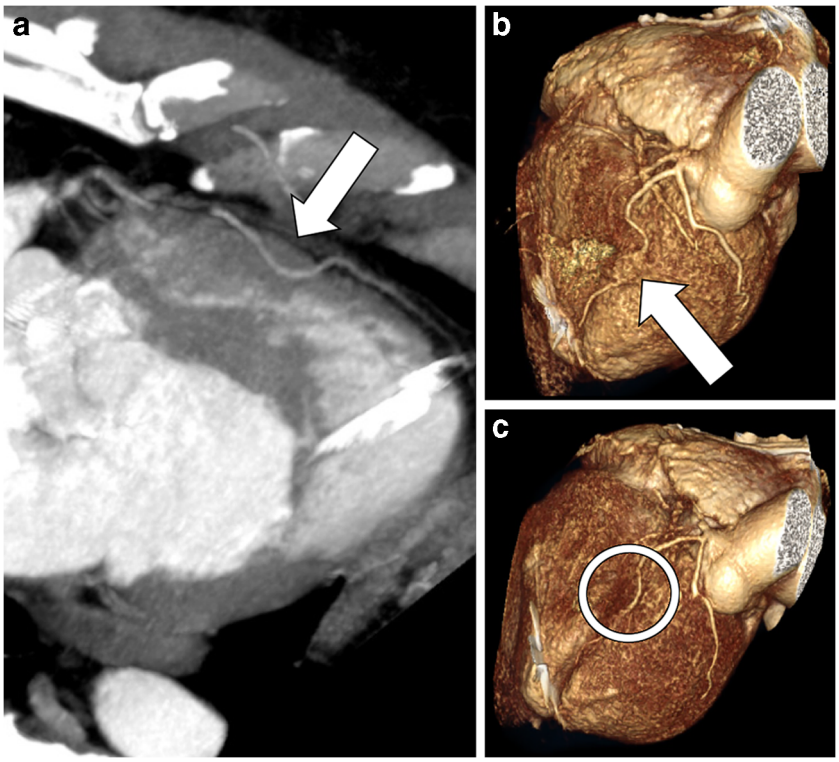

Fig. 6 Myocardial bridging in a 17-year-old boy. **a, b** Oblique sagittal maximum-intensity projection (**a**) and left anterior oblique volume-rendered (**b**) CT images reconstructed at end-systole show a myocardial muscular band overlying the middle segment of the left anterior descending artery with minimal luminal narrowing (*arrows*). **c** Left anterior oblique volume rendering displays the intramuscular course of the vessel after the overlying myocardium was removed (*circle*)

Anomalies of coronary termination essentially comprise coronary artery fistulas, which are communications of one or more coronary arteries, more commonly the right coronary artery, with a cardiac chamber, usually right-side structures such as the right ventricle, right atrium, pulmonary artery and coronary sinus. Coronary fistulas are very uncommon, being found in only 0.15% of people undergoing conventional angiography [50]. They are generally caused by embryological development disturbances but can also be acquired after trauma or invasive cardiac procedures [39]. The sites of origin and termination as well as the size of the abnormal connection have an impact on clinical significance. Most fistulas are small and without clinical implications, but large connections can entail significant left-to-right shunt and coronary artery steal, which can lead to ischemia of the portion of myocardium perfused by the coronary segment distal to the fistula. When present, clinical manifestations in adults include chest pain and dyspnea, whereas children are often asymptomatic. CT can provide 3-D anatomical images that help to confirm the diagnosis and better delineate the fistulous communications (Fig. 7), facilitating treatment planning as well as the detection of post-treatment complications, and potentially acting as a gatekeeper to invasive angiography, which can mainly be reserved for treatment [44].

Anomalies associated with congenital heart disease

Coronary artery abnormalities are more common in children with congenital heart disease. Even when clinically irrelevant, these lesions can become important because they can affect surgical repair [51]. Unambiguous coronary artery imaging is therefore mandatory in this situation and, especially when echocardiography is not conclusive, CT should be employed [52] to avoid unnecessary invasive procedures, even in the neonatal period. The most common conditions to consider in this setting include tetralogy of Fallot and (dextro-) transposition of the great arteries.

Tetralogy of Fallot is the most common cyanotic cardiac defect, defined by the classic tetrad of ventricular septal defect, overriding aorta, pulmonary outflow tract stenosis or atresia, and right ventricular hypertrophy. Complete repair involves ventriculotomy at the level of the right ventricular outflow tract. Consequently, ruling out an epicardial coronary vessel in that area prior to surgery is crucial. The most important abnormalities to recognize are anomalous origin of the left anterior descending artery from the right coronary artery with prepulmonary course, and a double left anterior descending artery, usually consisting of a short proximal vessel arising from the left coronary and a longer distal vessel arising from the right coronary that crosses the right outflow [53] (Fig. 8). Additionally, coronary artery anatomy should be known before repeat intervention on the outflow [54], repeat sternotomy to rule out substernal coronary course or transcatheter pulmonary valve placement to prevent coronary compression [52].

Transposition of the great arteries represents 5–7% of all forms of congenital heart disease and is characterized by ventriculo-arterial discordance, with origin of the aorta from the right ventricle and origin of the pulmonary trunk from the left ventricle, leading to cyanosis as

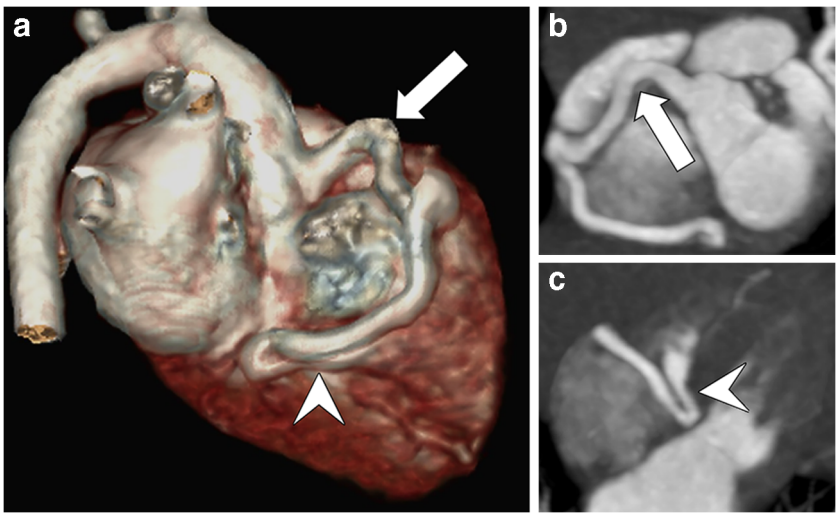

Fig. 7 Coronary artery fistula in a 1-year-old boy. **a–c** Right posterior volume-rendered (**a**), oblique coronal (**b**) and axial (**c**) maximum-intensity projection CT images show a large fistulous communication between the right coronary artery (*arrow*), which is dilated, and the right ventricle at the level of the crux cordis (*arrowhead*)

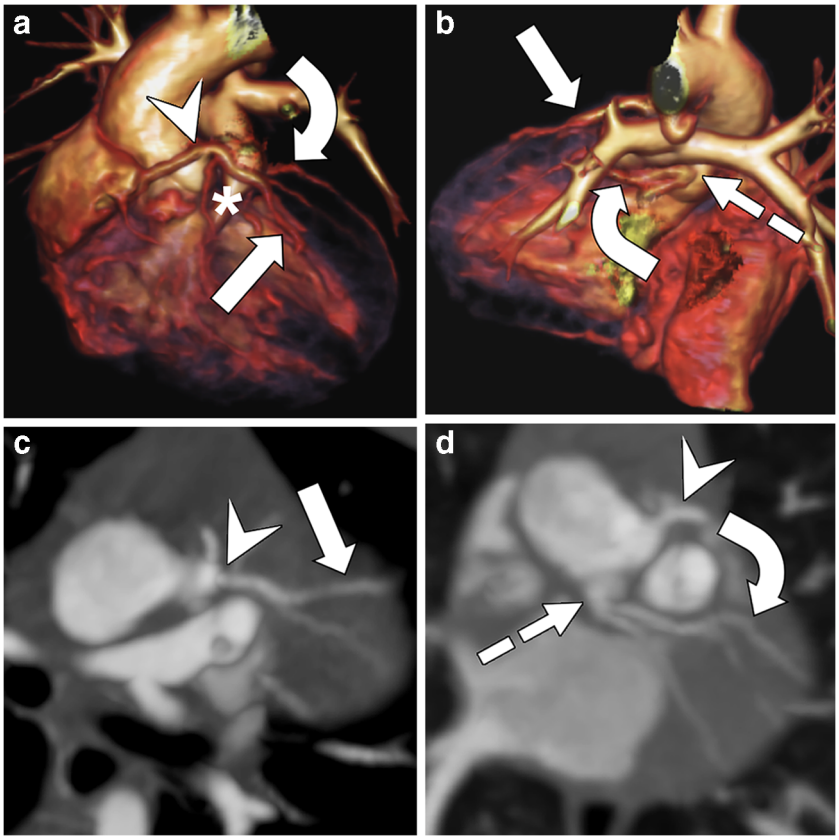

Fig. 8 Tetralogy of Fallot and double left anterior descending artery in a newborn boy. **a–d** Anterior (**a**) and posterior (**b**) volume-rendered, oblique axial (**c**) and oblique coronal (**d**) maximum-intensity projection CT images demonstrate a longer left anterior descending artery (*straight arrow*) arising from the right coronary (*arrowhead*) and coursing anteriorly to the stenotic right ventricular outflow tract (*asterisk*). There is also a shorter left anterior descending artery (*curved arrow*) coming off the left coronary (*dashed arrow*) and interrupting proximally but giving rise to diagonal branches

a result of two parallel circulations. Great vessel and coronary anatomy can be variable and have several classification systems [55]. Most commonly, the aorta is anterior and rightward relative to the pulmonary artery. Aortic sinuses are often described based on whether they are adjacent to the pulmonary artery, almost always bearing the coronary ostia, or not as facing and nonfacing, respectively. The most frequent coronary pattern involves the left coronary artery arising from the left anterior-facing sinus and the right coronary artery originating from the right posterior-facing sinus. Other notable arrangements include the left circumflex artery arising from the right coronary with a retropulmonary course (second most common), the left coronary coming off the right posterior-facing sinus with a retropulmonary course and the right coronary originating from the left anterior-facing sinus (inverted pattern), and single coronary artery [56]. Alternative classification schemes have been proposed where the aortic sinuses and coronary ostia are defined according to their relative location to the patient's axial anatomy and sequentially described [55]. Rarely, coronary course is intramural or interarterial (Fig. 9). Native coronary anatomy is a risk factor for the development of complications after surgical repair, particularly in people with single coronary orifice or intramural/interarterial course, who have a significantly increased mortality and higher rate of late adverse events [57].

Acquired coronary artery anomalies

Kawasaki disease

Kawasaki disease is a febrile systemic vasculitis of unknown origin that usually occurs in infancy and childhood. The acute phase is characterized by high fever, cutaneous rash, non-exudative conjunctivitis, oral mucosa inflammation, cervical adenopathy, swollen hands and feet, red palms and soles, and subungual peeling [58]. Acute cardiac manifestations include pericarditis, myocarditis, heart valve dysfunction and arrhythmias. About 15–25% of patients, especially when not treated early with high-dose intravenous immunoglobulins, develop

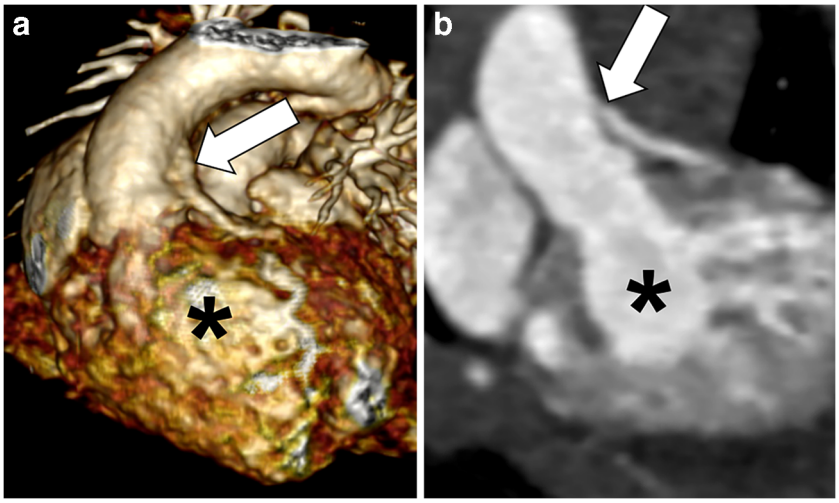

Fig. 9 Transposition of the great arteries and anomalous origin of the left coronary artery in a newborn girl. **a, b** Anterior volume-rendered (**a**) and coronal maximum-intensity projection (**b**) CT images show origin of the aorta from the right ventricle (*asterisk*) and high take-off of the left coronary artery, with likely proximal intramural course (*arrow*)

coronary artery aneurysms, which sometimes undergo thrombosis and progressive stenosis causing myocardial ischemia, infarction and sudden death [59]. Coronary aneurysms are more commonly located along the proximal left and right coronary arteries, but any segment can be affected. They can be saccular or fusiform, or there can be diffuse ectasia without segmental dilation. They can evolve over time in shape and size, increasing in dimension over the first 1–2 months after the onset of the disease and regressing in up to two-thirds of cases to normal lumen diameter within 2–5 years [60], with further regression being unlikely. Therefore, imaging follow-up of the coronary arteries is essential in these children. Echocardiography has high diagnostic accuracy for proximal aneurysms, but it is less sensitive for distal lesions and coronary artery stenosis, which usually worsens over time in the affected segments. For these reasons, CT is widely used to obtain high-resolution imaging of the whole coronary tree [4, 61] (Figs. 10 and 11), offering comparable accuracy to conventional angiography [62]. In case of giant aneurysms, repeating the scan at equilibrium contrast-phase might help to differentiate thrombosis from flow artifacts and depict persistent myocardial perfusion defects (Fig. 12).

Postoperative status

Surgical procedures employed for congenital coronary anomalies and heart disease entail coronary artery manipulation, leading to possible complications in the early and late postoperative course. In the setting of congenital heart disease, the most common interventions involving coronary reimplantation include the arterial switch operation for treating transposition of the great arteries and the Ross operation for managing aortic valve disease.

Since the early 1980s, the arterial switch operation has become the standard corrective technique for transposition in the absence of significant associated lesions like pulmonary stenosis [63]. The procedure re-creates physiological ventriculo-arterial concordance by transecting the great arteries and translocating them to the opposite root, with rearrangement of the pulmonary arteries anterior to the aorta (Lecompte maneuver). Translocation of the aorta implies mobilization and reimplantation of the coronary arteries, which are excised with a small cuff of aortic wall to be resutured into the neo-aortic root, with a somewhat stretched course compared to their original

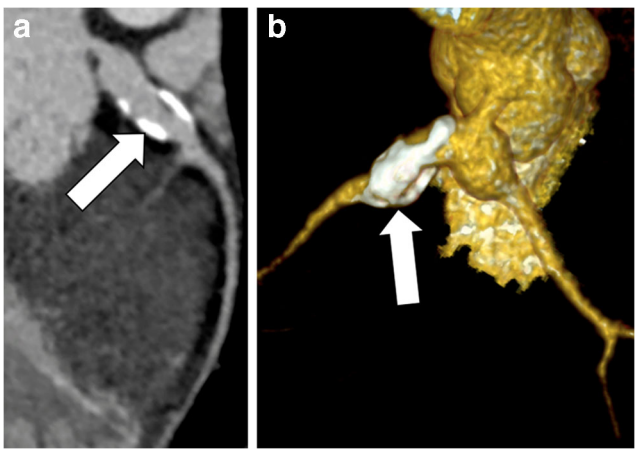

Fig. 10 Kawasaki disease in a 7-year-old girl. **a, b** Curved planar reformation (**a**) and left anterior volume-rendered (**b**) CT reconstructions show a large, partially calcified aneurysm of the left main coronary artery bifurcation (*arrow*)

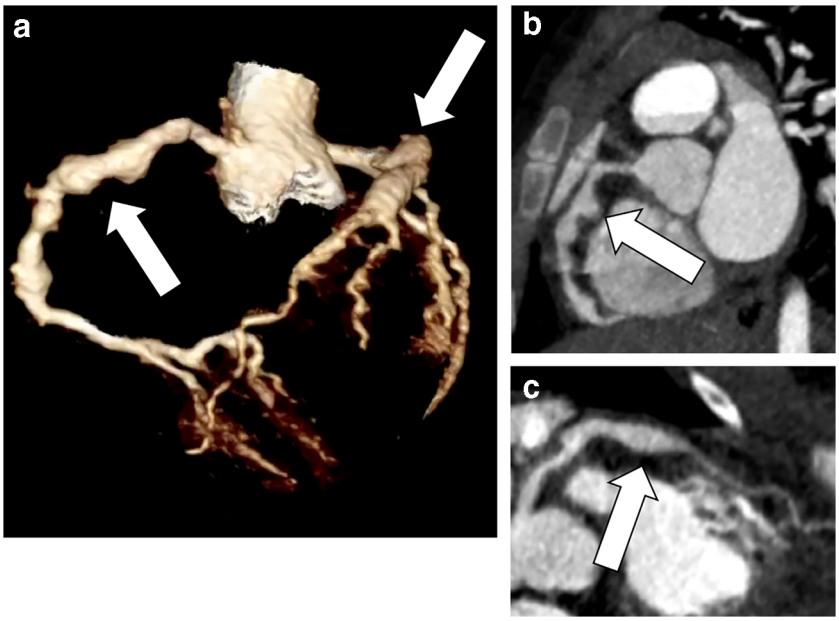

Fig. 11 Kawasaki disease in a 4-year-old boy. **a–c** Right anterior volume-rendered (**a**) and curved planar reformation CT views of the right (**b**) and the left (**c**) coronary arteries display diffusely beaded coronary arteries without significant obstruction (*arrows*)

Fig. 12 Kawasaki disease and giant aneurysms in a 2-year-old girl. **a** First-pass horizontal long-axis reformatted CT image documents a giant aneurysm of the middle right coronary artery with no visible lumen (*circle*) but cannot differentiate between thrombus and flow artifact. **b** Similar horizontal long-axis reconstruction at equilibrium contrast-phase confirms the finding, distinguishing between patent lumen (*arrowhead*) and eccentric thrombus (*arrow*). **c, d** Vertical long-axis (**c**) and mid-ventricular short-axis (**d**) views at equilibrium contrast-phase also demonstrate a persistent subendocardial perfusion defect of the left ventricular mid-basal inferior wall from ischemia/infarct (*arrows*)

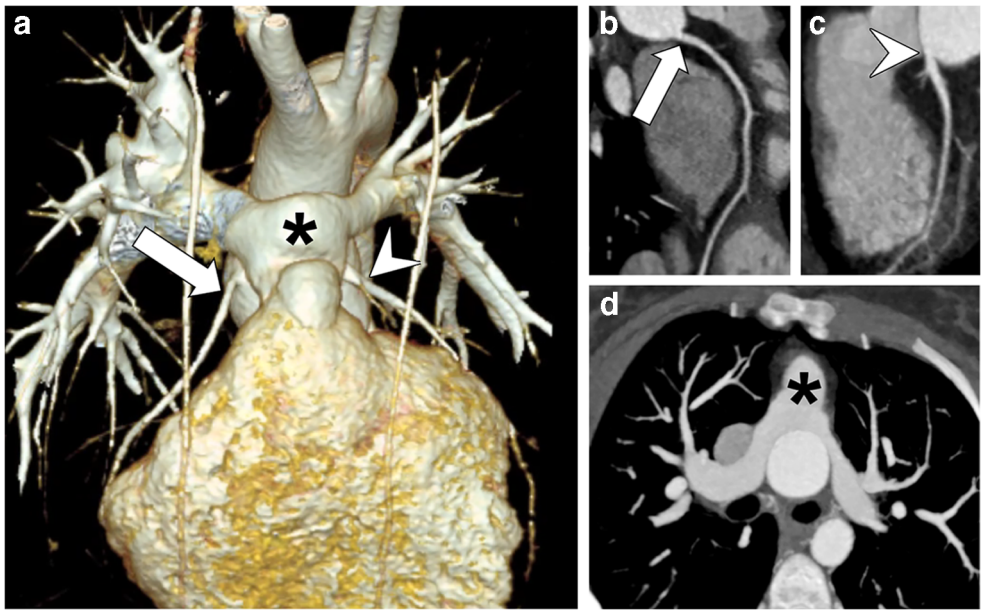

Fig. 13 Transposition of the great arteries after arterial switch operation in a 12-year-old girl. **a–d** Anterior oblique volume-rendered (**a**), curved planar reformation (**b, c**) and axial maximum-intensity projection (**d**) CT images show that the right (*arrow*) and left (*arrowhead*) coronary arteries are patent at the site of reimplantation. Note the typical anterior position of the pulmonary trunk (*asterisk*) relative to the aorta from the Lecompte maneuver

position (Fig. 13). In the early experiences, coronary manipulation was the main surgical issue, leading to coronary insufficiency and high perioperative mortality. Coronary transfer techniques have greatly improved since, with a substantial drop in hospital mortality, although the long-term success of the operation remains strictly dependent on the patency of the reimplanted coronary vessels. Most coronary events occur in the first 3 months after surgery [57] and are usually related to kinking or other types of anatomical obstruction to coronary perfusion. Late complications have an incidence of up to 10% and can lead to myocardial

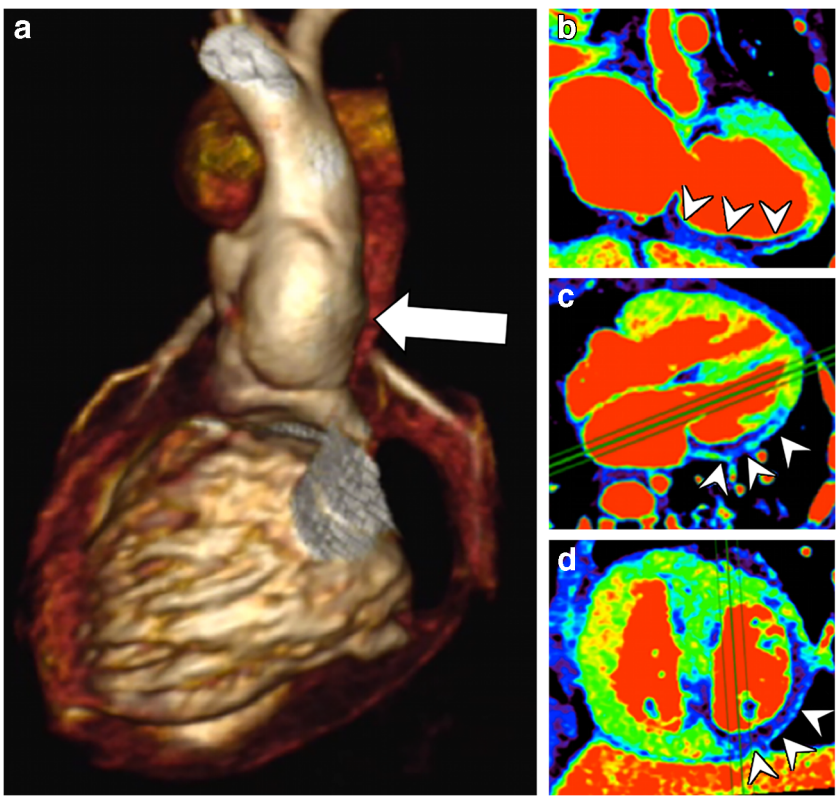

Fig. 14 Coronary complication after arterial switch operation in a 6-year-old girl. **a** Posterior volume-rendered CT image demonstrates that the dominant left circumflex artery is not opacified at the site of reimplantation (*arrow*). **b–d** Vertical (**b**) and horizontal (**c**) long-axis and mid-ventricular short-axis (**d**) CT reconstructions of color-coded perfusion maps confirm the finding by revealing a large transmural perfusion defect (*arrowheads*) in the infero-lateral wall, consistent with ischemic/infarcted myocardium

ischemia or infarction [64]. Imaging of coronary anastomoses is recommended in symptomatic children, as well as at least once in asymptomatic patients during adolescence or early adulthood [54]. Although catheter angiography is still the gold standard for coronary lesions, CT represents a reasonable alternative (Fig. 14), providing high-resolution imaging and reducing both the need and the risks of invasive studies such as coronary ostium alteration during catheter placement [65].

The Ross, or Ross-Konno, procedure is an alternative to prosthetic valve replacement in children with aortic valve stenosis [66]. During surgery, the pulmonary valve is translocated to the aortic position and a homograft conduit is placed to reestablish continuity from the right ventricle to the pulmonary artery. As with the arterial switch operation, the coronaries need to be excised from the native aortic sinuses and reimplanted into the neo-aortic root, but complications are less frequent because the vessels are reattached almost in their native position rather than being stretched (Fig. 15). Over recent years, other surgical operations implying coronary manipulation, such as the Nikaidoh procedure for people with transposition, ventricular septal defect and pulmonary stenosis, are becoming more common, expanding the potential indications for coronary artery follow-up by CT [52].

Finally, CT is useful to evaluate coronary artery bypass grafts and stents ≥3 mm in children with congenital or acquired heart disease undergoing revascularization [67] (Fig. 16) and to assess cardiac allograft vasculopathy in children post heart transplant [68]. CT has high sensitivity, specificity, and negative predictive values in these settings, comparable to invasive coronary angiography, and can be used during follow-up for detecting significant coronary artery lesions.

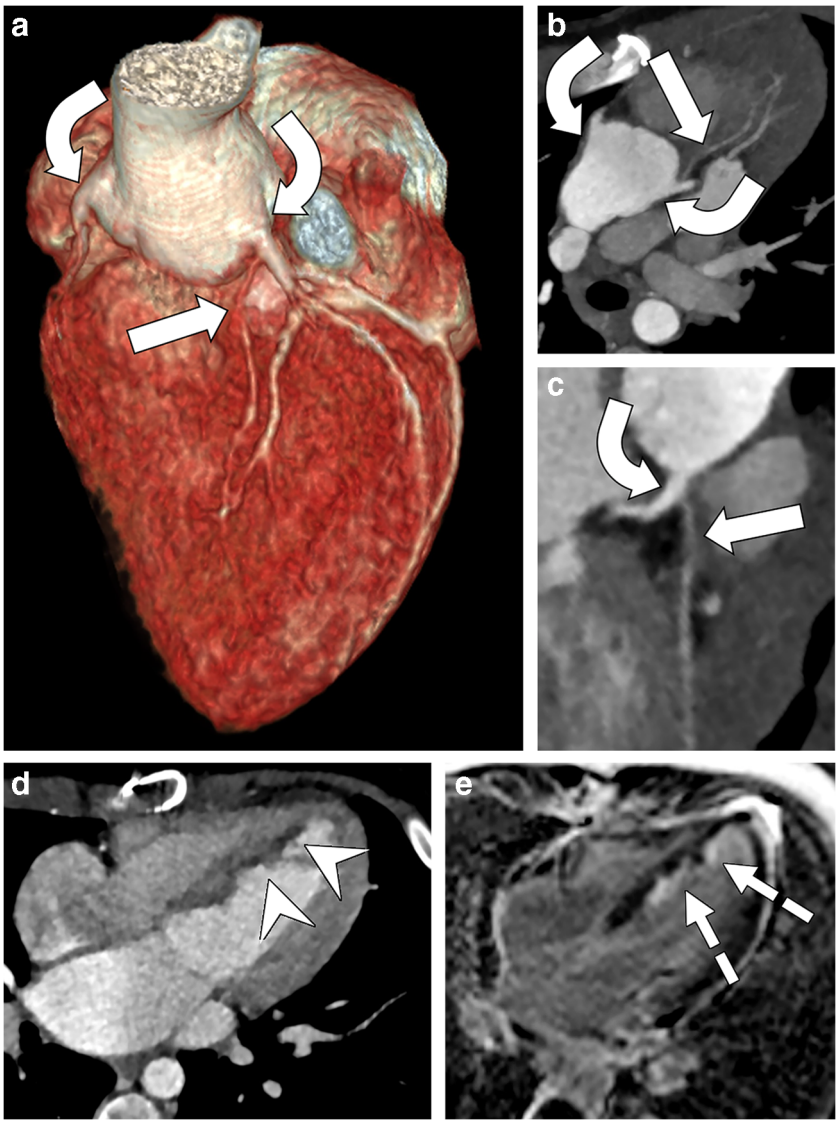

Fig. 15 Coronary complication after Ross operation in a 7-year old boy. **a-c** Left anterior oblique volume-rendered (**a**), oblique axial maximum-intensity projection (**b**) and curved planar reformation (**c**) CT images show that the coronary arteries are patent at the site of reimplantation (*curved arrows*) but the proximal portion of the left anterior descending artery is subocclusion (*straight arrow*). **d** Horizontal long-axis reconstruction documents a subendocardial perfusion defect in the septum and left ventricular apex (*arrowheads*). **e** Similar MRI late-gadolinium-enhancement image in the horizontal long-axis plane demonstrates a subendocardial infarct at the same level (*arrows*)

Fig. 16 Transposition of thegreat arteries after arterial switch operation and stenting of the proximal left anterior descending artery in a 14-year-old boy. **a, b** Curved planar reformat CT images of the stent demonstrate mild angulation of its proximal portion (a) and focal neointimal hyperplasia (*arrow*), significantly reducing the caliber of the stent lumen. **c, d** Curved planar reformat CT images of the stent obtained after percutaneous transluminal angioplasty show patency restoration of the stent lumen (*arrowhead*)

Conclusion

The technical improvements of dual-source CT represent a major advantage in the evaluation of children with coronary artery abnormalities because they allow for reliable assessment of small children with high heart rates by using low-dose protocols that minimize cardiac and respiratory motion artifacts and limit the need for sedation and anesthesia. These benefits enable the use of dual-source CT as a key technique in the workup of both congenital and acquired coronary anomalies in children, simultaneously opening new frontiers to expand current clinical indications.

Compliance with ethical standards

Conflicts of interest None

References

1. Lederlin M, Thambo JB, Latrabe V et al (2011) Coronary imaging techniques with emphasis on CT and MRI. Pediatr Radiol 41:1516–1525
2. Attili A, Hensley AK, Jones FD et al (2013) Echocardiography and coronary CT angiography imaging of variations in coronary anatomy and coronary abnormalities in athletic children: detection of coronary abnormalities that create a risk for sudden death. Echocardiography 30:225–233
3. Mehta R, Lee K-J, Chaturvedi R, Benson L (2008) Complications of pediatric cardiac catheterization: a review in the current era. Catheter Cardiovasc Interv 72:278–285
4. Goo HW (2015) Coronary artery imaging in children. Korean J Radiol 16:239–250
5. Han BK, Lindberg J, Grant K et al (2011) Accuracy and safety of high pitch computed tomography imaging in young children with complex congenital heart disease. Am J Cardiol 107:1541–1546
6. Han BK, Rigsby CK, Leipsic J et al (2015) Computed tomography imaging in patients with congenital heart disease, part 2: technical recommendations. An expert consensus document of the Society of Cardiovascular Computed Tomography (SCCT): endorsed by the Society of [sic] Pediatric Radiology (SPR) and the North American Society of [sic] Cardiac Imaging (NASCI). J Cardiovasc Comput Tomogr 9:493–513
7. Sigal-Cinqualbre A, Lambert V, Ronhean A, Paul JF (2011) Role of MSCT and MRI in the diagnosis of congenital heart disease. Arch Pediatr 18:617–627
8. Li J, Udayasankar UK, Toth TL et al (2007) Automatic patient centering for MDCT: effect on radiation dose. AJR Am J Roentgenol 188:547–552
9. Pache G, Grohmann J, Bulla S et al (2011) Prospective electrocardiography-triggered CT angiography of the great thoracic vessels in infants and toddlers with congenital heart disease: feasibility and image quality. Eur J Radiol 80:e440–e445
10. Booij R, Dijkshoorn ML, van Straten M et al (2016) Cardiovascular imaging in pediatric patients using dual source CT. J Cardiovasc Comput Tomogr 10:13–21
11. Han BK, Overman DM, Grant K et al (2013) Non-sedated, free breathing cardiac CT for evaluation of complex congenital heart disease in neonates. J Cardiovasc Comput Tomogr 7:354–360
12. Kim JW, Goo HW (2013) Coronary artery abnormalities in Kawasaki disease: comparison between CT and MR coronary angiography. Acta Radiol 54:156–163

13. Rigsby CK, deFreitas RA, Nicholas AC et al (2010) Safety and efficacy of a drug regimen to control heart rate during 64-slice ECG-gated coronary CTA in children. Pediatr Radiol 40:1880–1889
14. Mahabadi AA, Achenbach S, Burgstahler C et al (2010) Safety, efficacy, and indications of beta-adrenergic receptor blockade to reduce heart rate prior to coronary CT angiography. Radiology 257:614–623
15. Decramer I, Vanhoenacker PK, Sarno G et al (2008) Effects of sublingual nitroglycerin on coronary lumen diameter and number of visualized septal branches on 64-MDCT angiography. AJR Am J Roentgenol 190:219–225
16. Hopper KD, Mosher TJ, Kasales CJ et al (1997) Thoracic spiral CT: delivery of contrast material pushed with injectable saline solution in a power injector. Radiology 205:269–271
17. Goo HW (2013) Current trends in cardiac CT in children. Acta Radiol 54:1055–1062
18. Rigsby CK, Gasber E, Seshadri R et al (2007) Safety and efficacy of pressure-limited power injection of iodinated contrast medium through central lines in children. AJR Am J Roentgenol 188:726–732
19. Litmanovich D, Zamboni GA, Hauser TH et al (2008) ECG-gated chest CT angiography with 64-MDCT and tri-phasic IV contrast administration regimen in patients with acute non-specific chest pain. Eur Radiol 18:308–317
20. Fleischmann D (2003) High-concentration contrast media in MDCT angiography: principles and rationale. Eur Radiol 13: N39–N43
21. Stenzel F, Rief M, Zimmermann E et al (2014) Contrast agent bolus tracking with a fixed threshold or a manual fast start for coronary CT angiography. Eur Radiol 24:1229–1238
22. Machida H, Tanaka I, Fukui R et al (2015) Current and novel imaging techniques in coronary CT. Radiographics 35:991–1010
23. Nie P, Wang X, Cheng Z et al (2012) Accuracy, image quality and radiation dose comparison of high-pitch spiral and sequential acquisition on 128-slice dual-source CT angiography in children with congenital heart disease. Eur Radiol 22:2057–2066
24. Koh H, Ong CC, Choo YS et al (2016) Radiation dose and image quality in pediatric cardiac computed tomography: a comparison between sequential and third-generation dual-source high-pitch spiral techniques. Pediatr Cardiol 37:1397–1403
25. Paul J-F, Rohnean A, Elfassy E, Sigal-Cinqualbre A (2011) Radiation dose for thoracic and coronary step-and-shoot CT using a 128-slice dual-source machine in infants and small children with congenital heart disease. Pediatr Radiol 41:244–249
26. Li T, Zhao S, Liu J et al (2017) Feasibility of high-pitch spiral dual-source CT angiography in children with complex congenital heart disease compared to retrospective-gated spiral acquisition. Clin Radiol 72:864–870
27. Araoz PA, Kirsch J, Primak AN et al (2009) Optimal image reconstruction phase at low and high heart rates in dual-source CT coronary angiography. Int J Cardiovasc Imaging 25:837–845
28. Leipsic J, LaBounty TM, Ajlan AM et al (2013) A prospective randomized trial comparing image quality, study interpretability, and radiation dose of narrow acquisition window with widened acquisition window protocols in prospectively ECG-triggered coronary computed tomography angiography. J Cardiovasc Comput Tomogr 7:18–24
29. Pan C-J, Qian N, Wang T et al (2013) Adaptive prospective ECG-triggered sequence coronary angiography in dual-source CT without heart rate control: image quality and diagnostic performance. Exp Ther Med 5:636–642
30. Nakaura T, Kidoh M, Sakaino N et al (2013) Low contrast- and low radiation dose protocol for cardiac CT of thin adults at 256-row CT: usefulness of low tube voltage scans and the hybrid iterative reconstruction algorithm. Int J Cardiovasc Imaging 29:913–923
31. Litmanovich DE, Tack DM, Shahrzad M, Bankier AA (2014) Dose reduction in cardiothoracic CT: review of currently available methods. Radiographics 34:1469–1489
32. Lewis MA, Pascoal A, Keevil SF, Lewis CA (2016) Selecting a CT scanner for cardiac imaging: the heart of the matter. Br J Radiol 89: 20160376
33. Jadhav SP, Golriz F, Atweh LA et al (2015) CT angiography of neonates and infants: comparison of radiation dose and image quality of target mode prospectively ECG-gated 320-MDCT and ungated helical 64-MDCT. AJR Am J Roentgenol 204:W184–W191
34. Podberesky DJ, Angel E, Yoshizumi TT et al (2012) Radiation dose estimation for prospective and retrospective ECG-gated cardiac CT angiography in infants and small children using a 320-MDCT volume scanner. AJR Am J Roentgenol 199:1129–1135
35. Moscariello A, Takx RAP, Schoepf UJ et al (2011) Coronary CT angiography: image quality, diagnostic accuracy, and potential for radiation dose reduction using a novel iterative image reconstruction technique comparison with traditional filtered back projection. Eur Radiol 21:2130–2138
36. Abbara S, Blanke P, Maroules CD et al (2016) SCCT guidelines for the performance and acquisition of coronary computed tomographic angiography: a report of the Society of Cardiovascular Computed Tomography Guidelines Committee: endorsed by the North American Society for Cardiovascular Imaging (NASCI). J Cardiovasc Comput Tomogr 10:435–449
37. Leipsic J, Abbara S, Achenbach S et al (2014) SCCT guidelines for the interpretation and reporting of coronary CT angiography: a report of the Society of Cardiovascular Computed Tomography Guidelines Committee. J Cardiovasc Comput Tomogr 8:342–358
38. Karlo CA, Leschka S, Stolzmann P et al (2012) A systematic approach for analysis, interpretation, and reporting of coronary CTA studies. Insights Imaging 3:215–228
39. Zhang LJ, Zhou CS, Wang Y et al (2014) Prevalence and types of coronary to pulmonary artery fistula in a Chinese population at dual-source CT coronary angiography. Acta Radiol 55:1031–1039
40. Chao BT, Wang XM, Wu LB et al (2012) Diagnostic value of dual-source CT in Kawasaki disease. Chin Med J 123:670–674
41. Neves PO, Andrade J, Monção H (2015) Coronary anomalies: what the radiologist should know. Radiol Bras 48:233–241
42. Pursnani A, Jacobs JE, Saremi F et al (2012) Coronary CTA assessment of coronary anomalies. J Cardiovasc Comput Tomogr 6:48–59
43. Secinaro A, Ntsinjana H, Tann O et al (2011) Cardiovascular magnetic resonance findings in repaired anomalous left coronary artery to pulmonary artery connection (ALCAPA). J Cardiovasc Magn Reson 13:27
44. Agarwal PP, Dennie C, Pena E et al (2017) Anomalous coronary arteries that need intervention: review of pre- and postoperative imaging appearances. Radiographics 37:740–757
45. Kim SY, Seo JB, Do KH et al (2006) Coronary artery anomalies: classification and ECG-gated multi-detector row CT findings with angiographic correlation. Radiographics 26:317–333
46. Alegria JR, Herrmann J, Holmes DR et al (2005) Myocardial bridging. Eur Heart J 26:1159–1168
47. Hwang JH, Ko SM, Roh HG et al (2010) Myocardial bridging of the left anterior descending coronary artery: depiction rate and morphologic features by dual-source CT coronary angiography. Korean J Radiol 11:514–521
48. Ishikawa Y, Akasaka Y, Suzuki K et al (2009) Anatomic properties of myocardial bridge predisposing to myocardial infarction. Circulation 120:376–383
49. Husmann L, Nkoulou R, Wolfrum M, Kaufmann PA (2011) Myocardial bridging causing infarction and ischaemia. Eur Heart J 32:790

50. Said SA, el Gamal MI, van der Werf T (1997) Coronary arteriovenous fistulas: collective review and management of six new cases — changing etiology, presentation, and treatment strategy. Clin Cardiol 20:748–752
51. Yu FF, Lu B, Gao Y et al (2013) Congenital anomalies of coronary arteries in complex congenital heart disease: diagnosis and analysis with dual-source CT. J Cardiovasc Comput Tomogr 7:383–390
52. Han BK, Rigsby CK, Hlavacek A et al (2015) Computed tomography imaging in patients with congenital heart disease part i: rationale and utility. An expert consensus document of the Society of Cardiovascular Computed Tomography (SCCT): endorsed by the society of [sic] pediatric radiology (SPR) and the north American society of [sic] cardiac imaging (NASCI). J Cardiovasc Comput Tomogr 9:475–492
53. Agarwal PP, Kazerooni EA (2008) Dual left anterior descending coronary artery: CT findings. AJR Am J Roentgenol 191: 1698–1701
54. Warnes CA, Williams RG, Bashore TM et al (2008) ACC/AHA 2008 guidelines for the management of adults with congenital heart disease: a report of the American College of Cardiology/American Heart Association task force on practice guidelines (writing committee to develop guidelines on the management of adults with congenital heart disease). Circulation 118:e714–e833
55. Sithamparanathan S, Padley SP, Rubens MB et al (2013) Great vessel and coronary artery anatomy in transposition and other coronary anomalies: a universal descriptive and alphanumerical sequential classification. JACC Cardiovasc Imaging 6:624–630
56. Swanson SK, Sayyouh MM, Bardo DME et al (2018) Interpretation and reporting of coronary arteries in transposition of the great arteries: cross-sectional imaging perspective. J Thorac Imaging 33: W14–W21
57. Legendre A, Losay J, Touchot-Koné A et al (2003) Coronary events after arterial switch operation for transposition of the great arteries. Circulation 108:II186–II190
58. Newburger JW, Takahashi M, Gerber MA et al (2004) Diagnosis, treatment, and long-term management of Kawasaki disease: a statement for health professionals from the Committee on Rheumatic Fever, Endocarditis and Kawasaki Disease, Council on Cardiovascular Disease in the Young, American Heart Association. Circulation 110:2747–2771
59. Suda K, Iemura M, Nishiono H et al (2011) Long-term prognosis of patients with Kawasaki disease complicated by giant coronary aneurysms: a single-institution experience. Circulation 123: 1836–1842
60. Kato H, Sugimura T, Akagi T et al (1996) Long-term consequences of Kawasaki disease. A 10- to 21-year follow-up study of 594 patients. Circulation 94:1379–1385
61. Yu Y, Sun K, Wang R et al (2011) Comparison study of echocardiography and dual-source CT in diagnosis of coronary artery aneurysm due to Kawasaki disease: coronary artery disease. Echocardiography 28:1025–1034
62. Arnold R, Ley S, Ley-Zaporozhan J et al (2007) Visualization of coronary arteries in patients after childhood Kawasaki syndrome: value of multidetector CT and MR imaging in comparison to conventional coronary catheterization. Pediatr Radiol 37:998–1006
63. Gaca AM, Jaggers JJ, Dudley LT, Bisset GS 3rd (2008) Repair of congenital heart disease: a primer-part 1. Radiology 247:617–631
64. Bonhoeffer P, Bonnet D, Piéchaud JF et al (1997) Coronary artery obstruction after the arterial switch operation for transposition of the great arteries in newborns. J Am Coll Cardiol 29:202–206
65. Ou P, Celermajer DS, Marini D et al (2008) Safety and accuracy of 64-slice computed tomography coronary angiography in children after the arterial switch operation for transposition of the great arteries. JACC Cardiovasc Imaging 1:331–339
66. Laudito A, Brook MM, Suleman S et al (2001) The Ross procedure in children and young adults: a word of caution. J Thorac Cardiovasc Surg 122:147–153
67. Eichhorn JG, Jourdan C, Hill SL et al (2008) CT of pediatric vascular stents used to treat congenital heart disease. AJR Am J Roentgenol 190:1241–1246
68. Rohnean A, Houyel L, Sigal-Cinqualbre A et al (2011) Heart transplant patient outcomes: 5-year mean follow-up by coronary computed tomography angiography. Transplantation 91:583–588